ARROWHEAD CRATERS AND TOMAHAWK BASINS: SIGNATURES OF OBLIQUE IMPACTS AT LARGE SCALES. P. H. Schultz and A. M. Stickle, Department of Geological Sciences, Box 1846, Brown University, Providence, RI 02912 (peter_schultz@brown.edu).

Introduction: Crater excavation becomes less efficient with increasing scales and decreasing impact angles (with respect to the horizontal). Possible expressions of such changes in cratering efficiency include increasing amounts of melt [1] or increasing dimension of the central structure relative to the crater diameter [2,3]. Asymmetries in placement and shape of central relief suggest that the central uplift may preserve a signature of the initial trajectory and speed [3,4]. Such a suggestion provides an explanation for differences in central uplift styles (peak vs. peak-ring) for the same crater diameter on a given planetary body. The role of crustal structure [5] is a complementary, not a competing, hypothesis because crustal properties affect the penetration stage. In this study, it is proposed that projectile failure during oblique impacts plays an important role and becomes more evident at large scales due to reduction in crater diameter to projectile diameter, curvature (except at the largest scales), and impact speed.

Background: Oblique impacts in both laboratory and computational studies document the effects of projectile failure over a wide range of scales. In laboratory experiments, high-frame rate imaging and witness plates reveal the fate of the failed impactor, whether in gravity- or strength-controlled targets (e.g., aluminum). Downrange, ballistic fragments are localized in rays that subtend smaller angles with decreasing impact angles [6]. At very low impact angles (<20° from the horizontal), decapitated fragments also modify the downrange crater rim, creating what appears to be a double impact (**Fig. 1**). High-speed images reveal that these downrange fragments travel at speeds close to the initial impact speed and represent sheared fragments of the projectile. At high impact angles (or small scale), the transient crater may subsequently consume effects of this debris near the crater. Computational experiments also document this process at much larger scales (**Fig. 2**). At large scale and low impact angles, however, these features may not be lost during later excavation.

Large Scale Expressions: Formation of the transient crater diameter is largely controlled by both the energy and momentum coupled to the target, whereas melting and vaporization are primarily controlled by energy [1]. For oblique impacts, downward deformation (maximum penetration depth) is more controlled by momentum. Expressions of initial coupling include: (a) large offset central-peak or peak-ring diameters relative to crater diameter; (b) elongate central peak or elliptical central massif ring; and (c) breached peak-ring (downrange). These manifestations contrast with models where crater growth consumes all evidence of the initial stages of coupling. Nevertheless, it is a logical consequence of the reduced peak pressures created during an oblique impact. For reference, the ratio of the transient diameter to projectile diameter for an oblique at basin scales approaches the ratio for an oblique impact (15°) into solid aluminum.

It also has been suggested that elliptical basins are more likely to occur at basin scales due to the effect of surface curvature extending the coupling footprint [7,8]. Hence, an elliptical shape should be more common at larger scales. We propose here that such an elliptical shape is also modified by re-impacting parts of the sheared (decapitated) projectile. Because this process occurs at early times, the excavation stage overprints and masks surface expression at smaller scales, unless the impact is highly oblique [9,10] or accentuated by topographic effects. One example is the pear-shaped extension of the oblique impact crater Petavius-B on the Moon (trajectory from the northeast) and arrowhead-shaped craters on Mars [9,10].

Impact angle is expressed by proximal grooves and distal secondaries that change with azimuth and distance [11]. Downrange, distal grooves converge on the uprange edge of the basin, whereas proximal grooves (and extensions from secondary craters) converge closer to the basin center. This evolving pattern reflects the early-time flow field that becomes more apparent at large scales [11]. At large scales, expressions of the failed projectile also become more evident within the basin. The anvil-shaped or "tomahawk" outline of the inner breached massif ring of the Moscoviense (Fig. 3) and Crisium (Fig. 4) basins on the Moon (and the Hale basin on Mercury) illustrate possible expressions of downrange scouring by decapitated fragments.

For Crisium, the downrange extension (within the massif ring to the east) represents shallow excavation with linear valleys extending to either side [e.g., 4]. For Moscoviense, asymmetric grooves converge to the northwest (indicative of an oblique impact). Moscoviense also exhibits a breached interior ring and an extension to the northwest (along the proposed trajectory), which creates an anvil shape (**Fig. 3**). The central ring is offset uprange (southeast) with respect to the outer rings. At an even broader scale, the Orientale impact is an established oblique impact, based on the distribution of ejecta [11,12,13]. It also exhibits a bifurcated Inner Rooke to the southwest, consistent with the inferred trajectory from the

northeast with impactor debris directed to either side similar to Crisium (Fig.4). At much larger scales, sheared decapitated fragments may not interact with the surface due to surface curvature [11].

Implications: The identification of specific features associated with impactor coupling helps to constrain processes associated with the formation of large impact basins. Surviving projectile debris from major oblique impacts (e.g., Imbrium, Crisium, Mosoviense, and Orientale) also would have been dispersed at low angles and widely mixed with the early lunar crust, perhaps contributing to a missing component identified in the lunar highlands [14,15,16].

References: [1] Cintala, M.J., and R.A.F. Grieve, (1998), *Met. Planet. Sci.*, **33**, 889-912; [2] Schultz P.H. (1988), in *Mercury*, U. Arizona Press, Tucson, pp. 274-335; [3] Schultz, P.H. (1992), *J. Geophys. Res.*, **97**, No. E10, 16,183-16,248; [4] Schultz, P.H. (1996), *LPSC* 27, p.1147-1148; [5] Wieczorek, M. and Phillips, R. J. (1999), *Icarus*, **139**, June 1999, 246-25; [6] Schultz, P.H. and Gault, D.E. (1990), *Geol. Soc. Amer. Sp. Paper* **247**, 239-261; [7] Schultz, P.H. and Gault, D.E. (1992), *LPSC* 22 LPI, 1195-1196; [8] Andrews-Hannah, J. and Zuber, M.T. (2011), *Geol. Soc. Amer. Spec. Paper* 465 (in press); [9] Schultz P.H. and Lutz-Garihan A.B. (1982), *J. Geophys. Res.,* **87** *Supplement*, pp. A84-A96. [10] Chappelow, J. E. and Herrick, R. R. (2008), Icarus, *192*, 452-457; [11] Schultz P. H. and Papamarcos S. (2010), *LPSC* 41, abstract #2480; [12] McCauley, J. F (1977), *Phys. Earth Planet. Int*., **15**, 220-250; [13] Spudis, P. D. *et al.* (1989), *LPSC* 20,1042–1043; [14] Morgan, J.W. *et al*. (1974), *Proc. 5th Lunar Conf*, pp. 1703–1736; [15] Korotev, R.L. (1994), *Geochim. Cosmochim. Acta* **58**, 3931–3969; [16] Day et al. (2010), EPSL, **289**, 595-605; [17] Wrobel, K. and Schultz, P. H. (2008), *LPI Contrib.* No. 1353, p.3093.

Fig. 2: Results from a computation (CTH) of a 10° impact by a 25km dunite projectile into a basalt target 20 seconds after impact (modified from [17]). At such low angles, the decapitated projectile produces a downrange crater prior to excavation by the primary crater, thereby forming a double impact (arrow A). Relicts of the impactor are sprayed downrange subtending an angle close to twice the impact angle (arrow B) or scouring the surface (arrow C). At higher impact angles, crater growth may consume the downrange extension. At larger scales and lower impact angles, this feature may remain.

Fig.3: Lunar basin Moscoviense with "tomahawk-shaped" inner ring (dashed line) with downrange extensions characteristic of downrange impacts from the projectile. Highly degraded scours are identified to the NE.
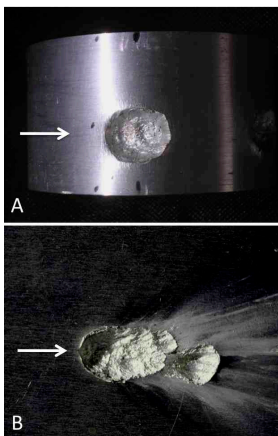

Fig. 1: Comparison of hypervelocity (5.2km/s) oblique impacts into an aluminum cylinder (A) and flat plate (B). Fragments from the decapitated projectile modify and extend the downrange crater rim for the flat plate target but not the cylinder (due to surface curvature). Note the scours in (B) that resulted from the decapitated impactor.
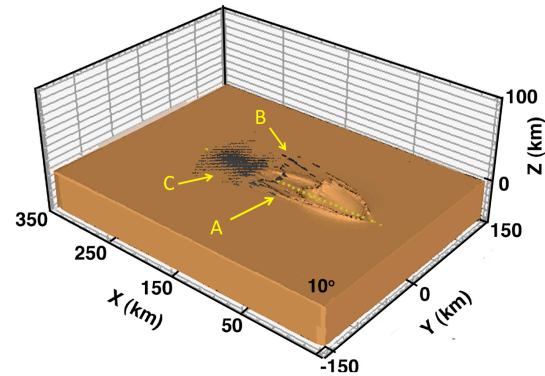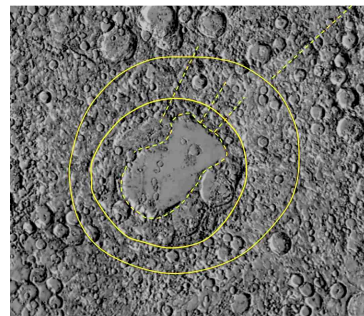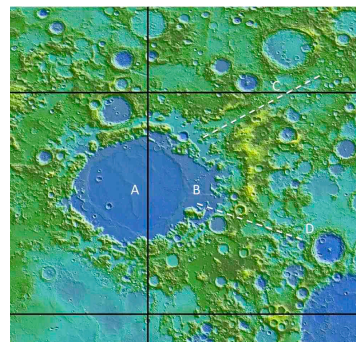

Fig.4: Lunar basin Crisium from LOLA topography. Elongate shape is attributed to an oblique trajectory (W to E) downrange (B). Grooves extend to either side (C and D) and are interpreted as scours (see Figs. 1 and 2).